Oscillatory double-diffusive convection in a rotating spherical shell at low Rayleigh numbers

Yue-Kin Tsang

School of Mathematics, Statistics and Physics
Newcastle University

Céline Guervilly, Graeme R. Sarson

Rayleigh–Bénard convection

$$\text{Density: } \rho(T) = \rho_m\big[1 - \alpha_T(T - T_m)\big], \qquad \alpha_T > 0$$

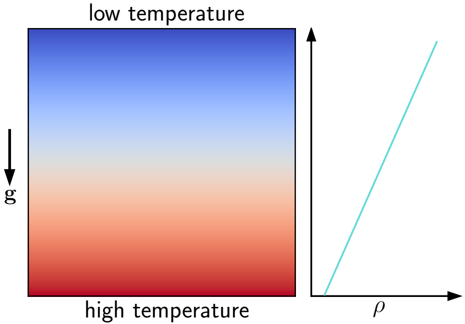

- at equilibrium ($\boldsymbol{u} = \mathbf{0}$): top-heavy
- T has a destabilising effect
- thermal Rayleigh number Ra_T is positive
- $Ra_T > Ra_0 \implies$ convection

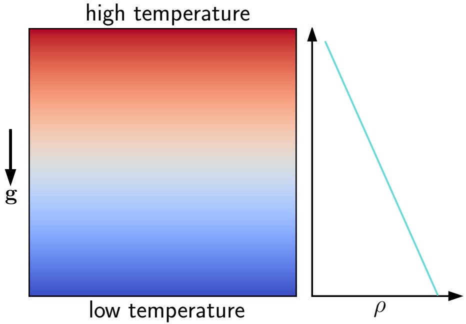

- at equilibrium, system is bottom-heavy
- T has a stabilising effect
- thermal Rayleigh number Ra_T is negative
- system is stable

Double-diffusive convection

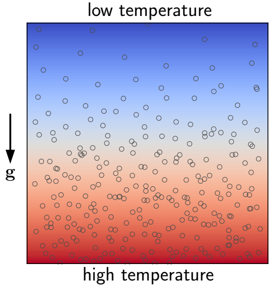

- density variation comes from two different components of the fluid
- consider a heavy element in the fluid, e.g. salt in seawater, He in H–He mixture
- let C be the concentration of the heavy element (composition):

$$\rho(T,C) = \rho_m\left[1 - \alpha_T(T - T_m) + \alpha_C(C - C_m)\right], \quad \alpha_T, \alpha_C > 0$$

- what distinguishes T and C is their diffusivities: $\kappa_T \gg \kappa_C$
- composition Rayleigh number: $Ra_C > 0 \implies$ destabilising, $Ra_C < 0 \implies$ stabilising

Different regimes of double-diffusive convection

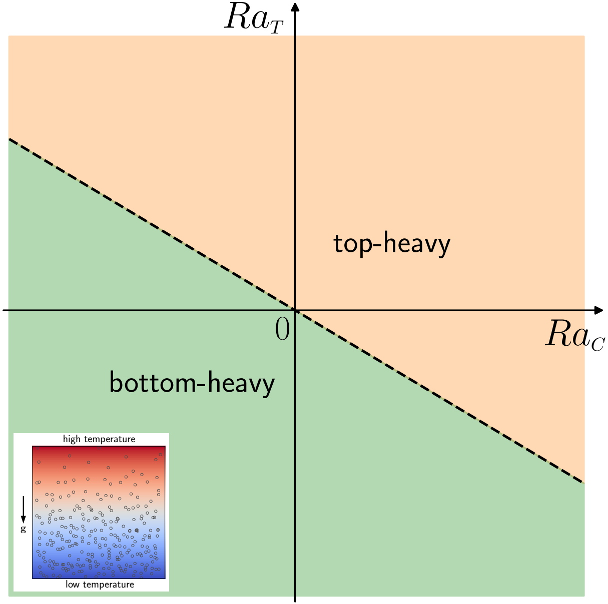

- stable

Different regimes of double-diffusive convection

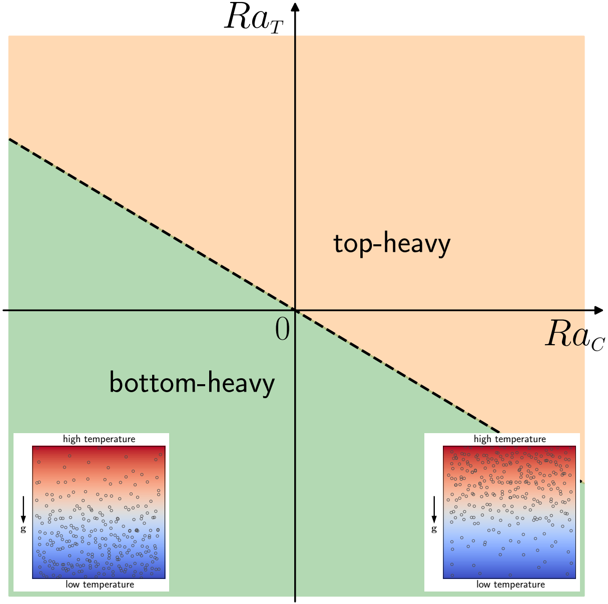

- stable

- e.g. upper ocean
- instabilities in stably-startified fluid
- salt fingers predicted by Stern(1960)

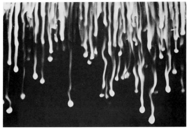

(Huppert & Turner 1981)

Different regimes of double-diffusive convection

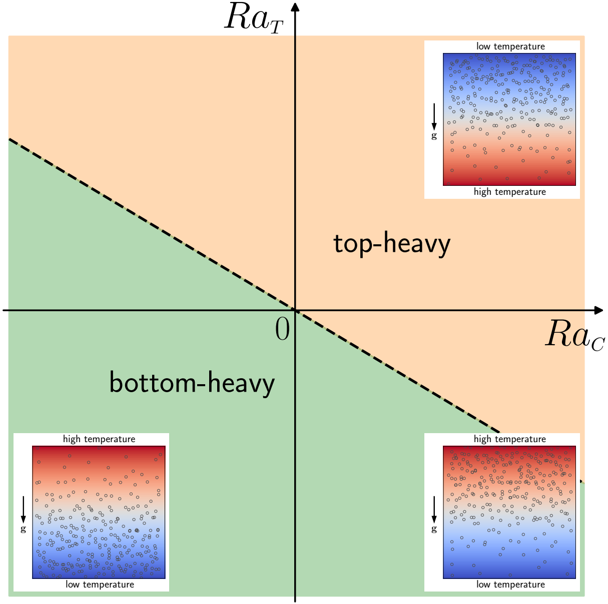

- stable

- e.g. Earth's outer core
- heavy iron solidifies onto the inner core
- excessive *light* elements at bottom

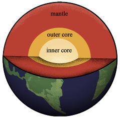

- e.g. upper ocean
- instabilities in stably-startified fluid
- salt fingers predicted by Stern(1960)

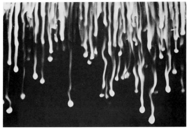

(Huppert & Turner 1981)

Different regimes of double-diffusive convection

- e.g. interior of Saturn
- diffusive convection
- semi-convection
- oscillatory double-diffusive convection (ODDC)

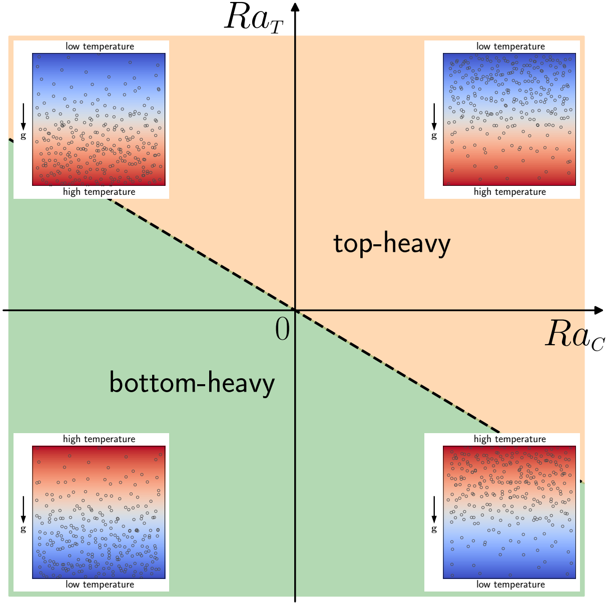

- stable

- e.g. Earth's outer core
- heavy iron solidifies onto the inner core
- excessive *light* elements at bottom

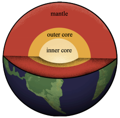

- e.g. upper ocean
- instabilities in stably-startified fluid
- salt fingers predicted by Stern(1960)

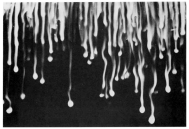

(Huppert & Turner 1981)

Possible scenarios of ODDC in planetary and stellar interiors

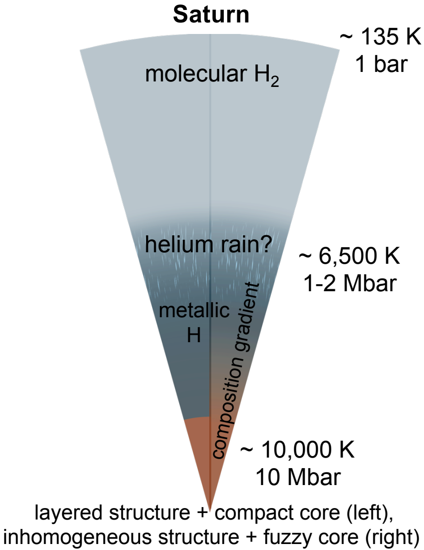

- Composition gradient may form inside Saturn in two different ways:
  - At some specific temperature and pressure, H and He become immiscible, heavier He forms droplets which fall towards the planetary interior—helium rain
  - Latest observations suggest Saturn may have a dilute/fuzzy core
- Composition gradient, and thus ODDC, may also exist in:
  - Jupiter
  - core-convective main sequence stars

Fortney et al. in "Saturn: The Grand Finale", K. H. Baines et al., eds., Cambridge University Press

Mathematical model: ODDC in a rotating spherical shell

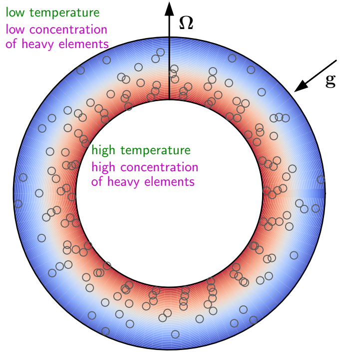

Boundary condition

fixed T gradient:

$$\left.\frac{\partial T}{\partial r}\right|_{r_i}, \left.\frac{\partial T}{\partial r}\right|_{r_o} < 0$$

fixed C gradient:

$$\left.\frac{\partial C}{\partial r}\right|_{r_i}, \left.\frac{\partial C}{\partial r}\right|_{r_o} < 0$$

Equilibrium profiles (at $\boldsymbol{u} = 0$)

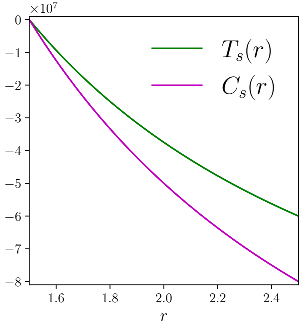

$\frac{\mathrm{d}T_s}{\mathrm{d}r} < 0$ *destabilising*

$\frac{\mathrm{d}C_s}{\mathrm{d}r} < 0$ *stabilising*

Consider a Boussinesq fluid in a rotating spherical shell of inner radius r_i and outer radius r_o

- composition diffusivity: $\kappa_C \ll \kappa_T$
- density: $\rho(T, C) = \rho_m[1 - \alpha_T(T - T_m) + \alpha_C(C - C_m)]$
- buoyancy frequency: $N^2 = -\frac{g}{\rho_m}\frac{\mathrm{d}}{\mathrm{d}r}[\rho(T_s, C_s)] \implies N^2 = g\alpha_T\frac{\mathrm{d}T_s}{\mathrm{d}r} - g\alpha_C\frac{\mathrm{d}C_s}{\mathrm{d}r}$

Governing equations

Non-dimensional equations:

$$\frac{\partial \boldsymbol{u}}{\partial t} + (\boldsymbol{u}\cdot\nabla)\boldsymbol{u} + \frac{2}{Ek}\hat{\boldsymbol{z}}\times\boldsymbol{u} = -\nabla\Pi + (\Theta - \xi) r\,\hat{\boldsymbol{r}} + \nabla^2\boldsymbol{u},$$

$$\nabla\cdot\boldsymbol{u} = 0,$$

$$\frac{\partial\Theta}{\partial t} + \boldsymbol{u}\cdot\nabla\Theta = \frac{Ra_T}{Pr}\left(\frac{\Gamma}{1-\Gamma}\right)^2\frac{u_r}{r^2} + \frac{1}{Pr}\nabla^2\Theta, \quad \Theta(\boldsymbol{x},t) = T(\boldsymbol{x},t) - T_s(r)$$

$$\frac{\partial\xi}{\partial t} + \boldsymbol{u}\cdot\nabla\xi = \frac{|Ra_C|}{Sc}\left(\frac{\Gamma}{1-\Gamma}\right)^2\frac{u_r}{r^2} + \frac{1}{Sc}\nabla^2\xi, \quad \xi(\boldsymbol{x},t) = C(\boldsymbol{x},t) - C_s(r)$$

Dimensionless numbers:

$$\Gamma = \frac{r_i}{r_o} = 0.6, \quad Ek = \frac{\nu}{\Omega D^2} = 10^{-5}, \quad \text{(small)}\ Pr = \frac{\nu}{\kappa_T} = 0.3, \quad Sc = \frac{\nu}{\kappa_C} = 3 \quad \left(\tau = \frac{\kappa_C}{\kappa_T} = 0.1\right)$$

$$Ra_T = \frac{g_o\alpha_T D^5}{r_o\nu\kappa_T}\left|T_s'(r_i)\right| \quad \text{and} \quad Ra_C = -\frac{g_o\alpha_C D^5}{r_o\nu\kappa_C}\left|C_s'(r_i)\right|$$

Numerical simulations using XSHELLS by Nathanaël Schaeffer (Université Grenoble Alpes, CNRS)

ODDC at low Rayleigh numbers

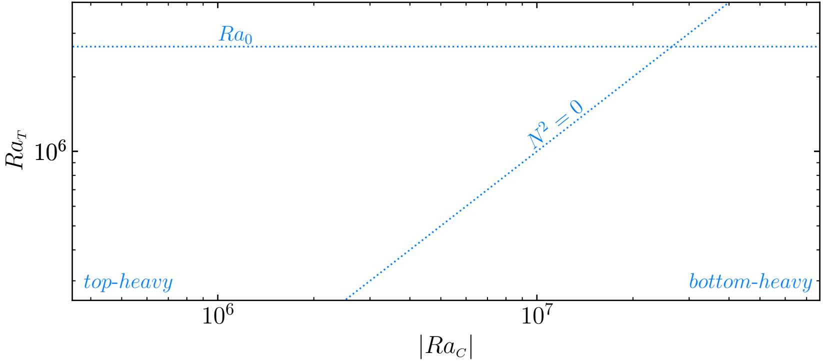

- (non-dimensional) $N^2 = -\frac{Ra_T}{Pr}\frac{r_i^2}{r} + \frac{|Ra_C|}{Sc}\frac{r_i^2}{r}$

  $N^2 < 0$: unstable stratification, $\quad N^2 > 0$: stably stratified

- Ra_0 = critical Rayleigh number for pure thermal convection

  pure thermal convection: unstable when $N^2 < 0$ and $Ra_T > Ra_0$

Phase diagram: stability

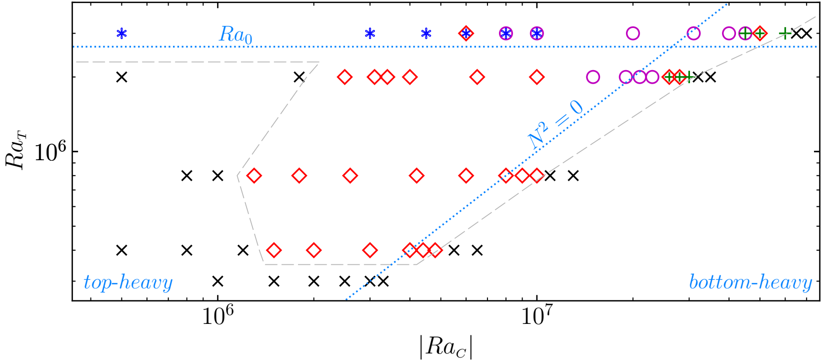

black crosses ($\times$) $\Longrightarrow$ stable   coloured symbols ($*, +, \diamond, \circ$) $\Longrightarrow$ unstable

- Despite the equilibrium composition gradient $\mathrm{d}C_s/\mathrm{d}r$ is stabilising:
  - convection occurs for some $Ra_T < Ra_0$ (= critical Rayleigh number for thermal convection)
  - system can become unstable even when $N^2 > 0$
- This counter-intuitive phenomenon only happens for an intermediate range of $|Ra_C|$

Flow patterns: $Ra_T > Ra_0$ and intermediate $|Ra_C|$

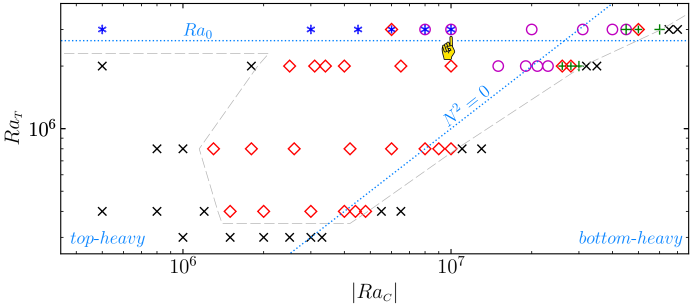

$$Ra_T = 3.0 \times 10^6$$
$$|Ra_C| = 1.0 \times 10^7$$

- fast small-scale thermal-Rossby-like spirals coexist with slow large-scale structures
- the two components drift in opposite direction
- modulated spiral columns in localised spots

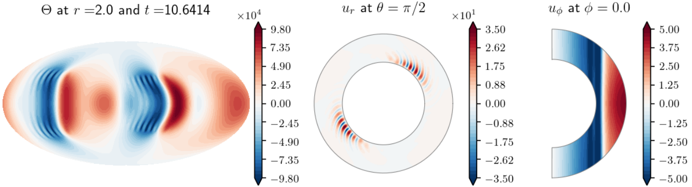

Thin cylindrical annulus model (Busse 1986)

Trim the spherical shell into a cylindrical annulus . . .

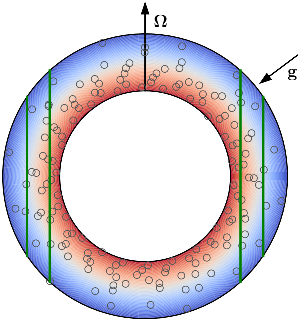

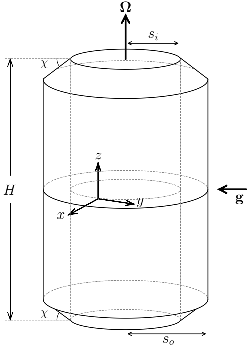

- top and bottom of the cylindrical annulus tilted at a constant angle χ
- temperature and composition gradients decrease with radius
- captures two pieces of physics of the spherical shell:
    1. rapid rotation
    2. curvature of the spherical geometry

Thin cylindrical annulus model (Busse 1986)

Flatten the cylindrical annulus into a plane . . .

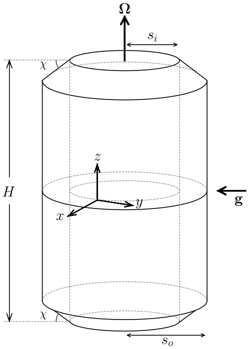

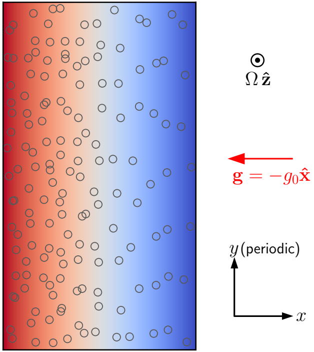

- rapid rotation $\Rightarrow$ geostrophic balance at leading order (columnar structures)
- integration over height + tilted boundaries $\Rightarrow$ two-dimensional system with β-effect
- thin annulus $\Rightarrow$ Cartesian coordinate: radial $\rightarrow x$, azimuthal $\rightarrow y$ (periodic)

ODDC on a two-dimensional β-plane

2D-velocity (u, v) in terms of a streamfunction ψ:

$$(u, v) = \big(-\partial_y \psi, \partial_x \psi \big)$$

Define the Jacobian:

$$J(A, B) = \partial_x A \, \partial_y B - \partial_y A \, \partial_x B$$

Governing equations for (ψ, Θ, ξ):

$$\frac{\partial}{\partial t} \nabla^2 \psi + J(\psi, \nabla^2 \psi) - \beta \frac{\partial \psi}{\partial y} = -\frac{\partial}{\partial y} (\Theta - \xi) + \nabla^4 \psi$$

$$\frac{\partial \Theta}{\partial t} + J(\psi, \Theta) = -\frac{Ra_T}{Pr} \frac{\partial \psi}{\partial y} + \frac{1}{Pr} \nabla^2 \Theta$$

$$\frac{\partial \xi}{\partial t} + J(\psi, \xi) = -\frac{|Ra_C|}{Sc} \frac{\partial \psi}{\partial y} + \frac{1}{Sc} \nabla^2 \xi$$

$$\beta = \frac{4 \, \Gamma \tan \chi}{Ek}$$

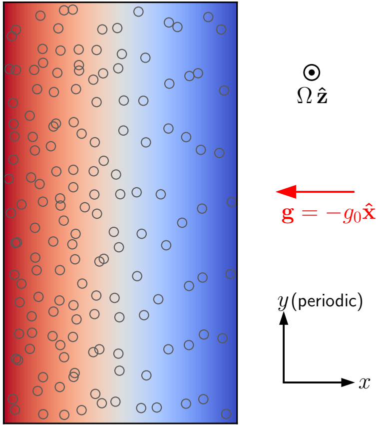

Busse, *Geophysical Research Letters* **29**, 1105 (2002)

Simitev, *Physics of the Earth and Planetary Interiors* **186**, 183 (2011)

Linear stability analysis

Linearised equations (+ boundary conditions):

$$\frac{\partial}{\partial t}\nabla^2\psi - \beta\frac{\partial\psi}{\partial y} = -\frac{\partial\Theta}{\partial y} + \frac{\partial\xi}{\partial y} + \nabla^4\psi$$

$$\frac{\partial\Theta}{\partial t} = -\frac{Ra_T}{Pr}\frac{\partial\psi}{\partial y} + \frac{1}{Pr}\nabla^2\Theta$$

$$\frac{\partial\xi}{\partial t} = -\frac{|Ra_C|}{Sc}\frac{\partial\psi}{\partial y} + \frac{1}{Sc}\nabla^2\xi$$

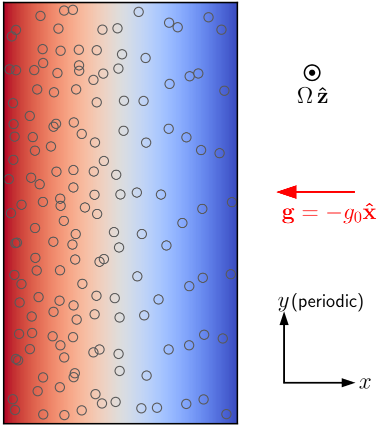

Eigenfunctions: modes with wavenumber (k, l),

$$\psi(x,y,t) = \hat{\psi}\sin(kx)\,e^{ily}\,e^{\lambda t}$$

$$\Theta(x,y,t) = \hat{\Theta}\cos(kx)\,e^{ily}\,e^{\lambda t}$$

$$\xi(x,y,t) = \hat{\xi}\cos(kx)\,e^{ily}\,e^{\lambda t}$$

Eignevalues: complex growth rate,

$$\lambda = \sigma + i\omega \quad (\sigma, \omega \in \mathbb{R})$$

Maximum growth rate and neutral curve

Solvability condition gives the equation for the eigenvalue $\lambda = \sigma + i\omega$:

$$\lambda^3 + \left(\frac{1+Pr+\tau}{Pr}k_\mathrm{h}^2 + i\frac{\beta l}{k_\mathrm{h}^2}\right)\lambda^2 + \left[\frac{Pr+\tau(1+Pr)}{Pr^2}k_\mathrm{h}^4 + \frac{\tau|Ra_C| - Ra_T}{Pr}\frac{l^2}{k_\mathrm{h}^2} + i\frac{\beta(1+\tau)}{Pr}l\right]\lambda + \frac{\tau}{Pr^2}\left[k_\mathrm{h}^6 + (|Ra_C| - Ra_T)l^2 + i\beta k_\mathrm{h}^2 l\right] = 0$$

$(k,l) = (m\pi, \frac{n}{s_i})$, $m,n \in \mathbb{Z}$, $\quad k_\mathrm{h}^2 \equiv k^2 + l^2$, $\quad Pr = 0.3$, $\quad \tau = Pr/Sc = 0.1$, $\quad \beta = 1.78 \times 10^5$

- A cubic equation $\Longrightarrow$ three roots: $\lambda_q = \sigma_q + i\omega_q$, $q = 1,2,3$

1. For each (Ra_T, Ra_C), maximum growth rate $\sigma^{\max}(Ra_C, Ra_T)$:

$$\sigma_q^{\max}(Ra_C, Ra_T) = \max_{k,l}\left\{\sigma_q(k,l\,;Ra_C, Ra_T)\right\}, \quad q = 1,2,3$$

$$\sigma^{\max}(Ra_C, Ra_T) = \max_q\left\{\sigma_q^{\max}\right\}$$

2. Setting $\sigma = 0$, we can trace the stability boundary (neutral curve) on the Ra_T–Ra_C phase plane

Maximum growth rate and neutral curve

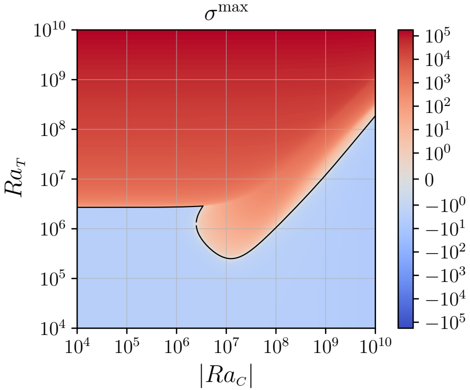

- Similar qualitative features as in the stability diagram for the spherical shell
- We can learn more by taking a step back and investigating each $\sigma_q^{\max}$ individually

$$\sigma^{\max}(Ra_C, Ra_T) = \max_q \left\{\sigma_q^{\max}\right\}, \quad q = 1, 2, 3$$

- There is always a decaying solution: $\sigma_2^{\max} < 0$

Composition modified thermal-Rossby mode: $\sigma_1^{\max}$

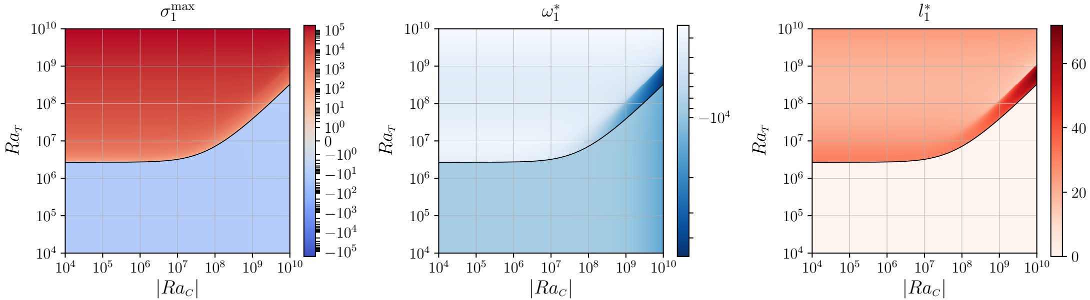

$Ra_{0,2d}$ = critical Ra of pure thermal convection on a β-plane

- unstable only when $Ra_T > Ra_{0,2d}$
- optimal frequency $\omega_1^* < 0 \implies$ prograde
- high optimal wavenumber: $l_1^* \gtrsim 30 \implies$ small-scale
- $\sim$ thermal-Rossby waves in pure thermal convection (slightly modified by the stabilising effects of the compositional)

Double-diffusive mode: $\sigma_3^{\max}$

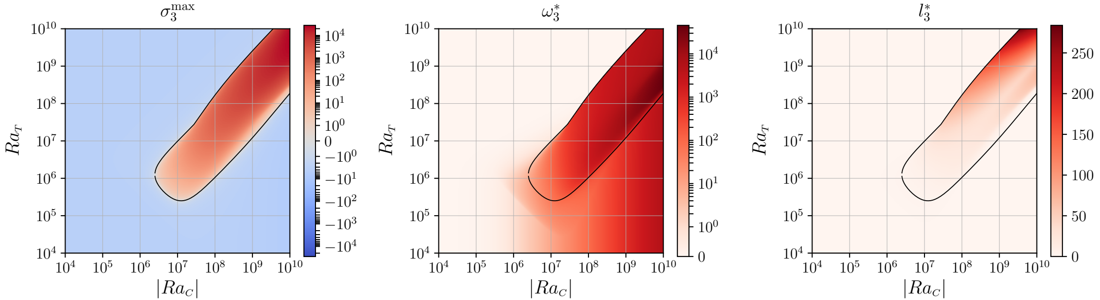

$Ra_{0,2d}$ = critical Ra of pure thermal convection on a β-plane

- instability region extends below $Ra_{0,2d}$
- optimal frequency $\omega_3^* > 0 \implies$ retrograde
- low optimal wavenumber: $l_3^* \sim 1$ within the 'tongue' $\implies$ large-scale
- a genuine double-diffusive mode

Superposition of different modes

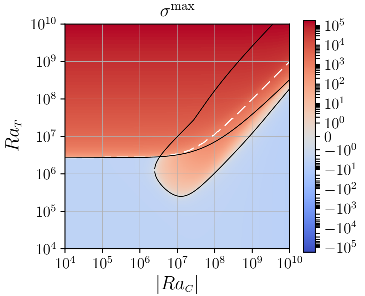

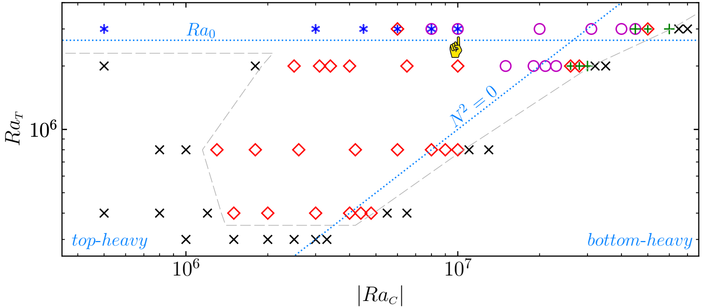

- 2D linear stability analysis: there is a region where both the thermal-Rossby-like mode and the double-diffusive mode can grow
- Nonlinear simulation: the two modes coexist with minimal interaction (low Ra_T, weakly nonlinear)